

# A JOINT FRAMEWORK FOR 4D SEGMENTATION AND ESTIMATION OF SMOOTH TEMPORAL APPEARANCE CHANGES

Yang Gao<sup>1</sup>, Marcel Prastawa<sup>1</sup>, Martin Styner<sup>2</sup>, Joseph Piven<sup>2</sup> for IBIS\*, Guido Gerig<sup>1</sup>

<sup>1</sup>Scientific Computing and Imaging Institute  
School of Computing, University of Utah  
Salt Lake City, UT 84112

<sup>2</sup>Department of Psychiatry  
University of North Carolina  
Chapel Hill, NC 27599

## ABSTRACT

Medical imaging studies increasingly use longitudinal images of individual subjects in order to follow-up changes due to development, degeneration, disease progression or efficacy of therapeutic intervention. Repeated image data of individuals are highly correlated, and the strong causality of information over time lead to the development of procedures for joint segmentation of the series of scans, called 4D segmentation. A main aim was improved consistency of quantitative analysis, most often solved via patient-specific atlases. Challenging open problems are contrast changes and occurrence of subclasses within tissue as observed in multimodal MRI of infant development, neurodegeneration and disease. This paper proposes a new 4D segmentation framework that enforces continuous dynamic changes of tissue contrast patterns over time as observed in such data. Moreover, our model includes the capability to segment different contrast patterns within a specific tissue class, for example as seen in myelinated and unmyelinated white matter regions in early brain development. Proof of concept is shown with validation on synthetic image data and with 4D segmentation of longitudinal, multimodal pediatric MRI taken at 6, 12 and 24 months of age, but the methodology is generic w.r.t. different application domains using serial imaging.

## 1. INTRODUCTION

Longitudinal analysis of MR images has great potential to reveal the development patterns of brain growth, deviation from normal trajectories, monitoring disease progress and/or

effects of therapeutic intervention, and studies of neurodegeneration in aging. Accurate and consistent segmentation of longitudinal image sequences is a key processing step to better understand even subtle temporal changes of anatomy. Recent work demonstrated that joint segmentation of serial imaging can lead to improved analysis of spatiotemporal patterns of change since 4D procedures optimally use the inherent correlation of repeated scans of individual subjects. Current methodologies still show significant challenges related to temporal variations in image appearance due to differences in scanner calibrations, global or local tissue changes related to development or aging, and appearance variations related to disease. Reuter et al. [1] introduce a FreeSurfer longitudinal analysis framework based on unbiased within-subject template creation to reduce variability of segmentation in each time point. Kim et al. [2] focus on brain maturation and related contrast changes and developed a spatial intensity growth map (IGM) that compensates for the white matter intensity appearance inhomogeneity. Shi et al. [3] take advantage of the fact that MRI presents improved tissue contrast at older age and proposed the use of a subject-specific tissue probability atlas to guide segmentation at earlier time points. Xue et al. [4] propose an image-adaptive clustering, spatiotemporal smoothness constraints, and image warping to jointly segment same subject serial MRI. The clustering objective function treats the spatially and temporally adaptive smoothness constraints in a similar manner despite significant differences across space and time. Prastawa et al. [5] present a framework for construction of subject-specific longitudinal anatomical models including joint segmentation, registration and personalized atlas building, with individual Gaussian mixture model per time point to account for temporal contrast differences. Regularization over time is achieved via kernel smoothing of the longitudinal subject-specific tissue probability atlas.

Whereas most previously reported methods focused on improving consistency of segmentation of serial image data of same types of contrast to tackle random variations, this paper provides a new solution to explicitly model temporal brain tissue appearance changes inherent to biological variations as seen in development, degeneration or disease pro-

---

This work is supported by NIH grants ACE RO1 HD 055741, Twin R01 MH070890, Conte Center MH064065 and NA-MIC Roadmap U54 EB005149. \*The NIH funded Autism Centers of Excellence Infant Brain Imaging Study (ACE-IBIS) Network: Clinical Sites: University of North Carolina: J. Piven (IBIS Network PI), H.C. Hazlett, C. Chappell; University of Washington: S. Dager, A. Estes, D. Shaw; Washington University: K. Botteron, R. McKinstry, J. Constantino, J. Pruett; Children's Hospital of Philadelphia: R. Schultz, S. Paterson; University of Alberta: L. Zwaigenbaum; Data Coordinating Center: Montreal Neurological Institute: A.C. Evans, D.L. Collins, G.B. Pike, V. Fonov, P. Kostopoulos; Samir Das; Image Processing Core: University of Utah: G. Gerig; University of North Carolina: M. Styner; Statistical Analysis Core: University of North Carolina: H. Gu.

gression. Assuming co-registered sets of images, our method models voxel-wise time-related intensity changes through the entire time series of individual subjects and is designed to process longitudinal multimodality data such as shown in [6]. We define an objective function on the temporal intensity change model and solve 4D segmentation via nonlinear optimization.

The driving application is the segmentation of multimodal brain MRI during the first 2 years of life, with the well known challenges of reversal and disappearance of white and gray matter contrast, spatial tissue appearance inhomogeneities, and rapidly changing regional maturation of non-myelinated to myelinated white matter. Proof of concept is shown on both simulated longitudinal data and clinical longitudinal pediatric brain MRI. However, the proposed method is not limited to pediatric imaging but to all scenarios where serial images show large contrast changes and inhomogeneities.

## 2. METHOD

Let us consider a longitudinal MRI sequence of a single subject, acquired at multiple time points  $t \in \{1, \dots, T\}$  and assume that all images are co-registered via pre-processing not discussed as part of this work. Each image  $\mathbf{I}^t = \{\mathbf{I}^t(x) : x \in \mathbb{R}^3\}$  in the sequence has anatomical structures characterized by total  $C$  categories. Voxel-wise segmentation requires well-separated modes in multi-modal intensity distributions. One common problem we meet in longitudinal image segmentation of MRI in scenarios of brain changes is that some time points show well-separated intensity distributions whereas others do not. Another problem is the presence of regional tissue inhomogeneities or even existence of several property types related to biological changes, significantly changing over the time series and appearing homogeneous at certain time points. In this case, several modes in the intensity distributions of a tissue category at a few time point merge to a single mode at another time point. Fig. 1 illustrates the key ideas of our intensity modeling to conquer these problems.

### 2.1. Intensity Change Model

Assuming aligned images and smooth temporal growth, the intensities of a voxel at location  $x$  through all time points should show a systematic relationship. Ideally, intensities would be more similar for voxels at neighboring time points than further apart. In reality, this may not be the case due to types of changes discussed previously, motivating the use of an intensity adjustment in addition to an ideal smooth model fit. To model temporal relationships via intensity similarities, we define an intensity change  $\phi^t(x)$  of original voxel intensities  $\mathbf{I}^t(x)$  at every time point  $t$  and location  $x$ . After adjustment, the new intensity  $\mathbf{I}^{t_i}(x) + \phi^{t_i}(x)$  at time point  $t_i$  should be similar to the new intensity  $\mathbf{I}^{t_j}(x) + \phi^{t_j}(x)$  at time point  $t_j$ . We use a similarity metric which satisfies closer similarity with smaller time distance  $|t_i - t_j|$ , i.e. smaller intensities dif-

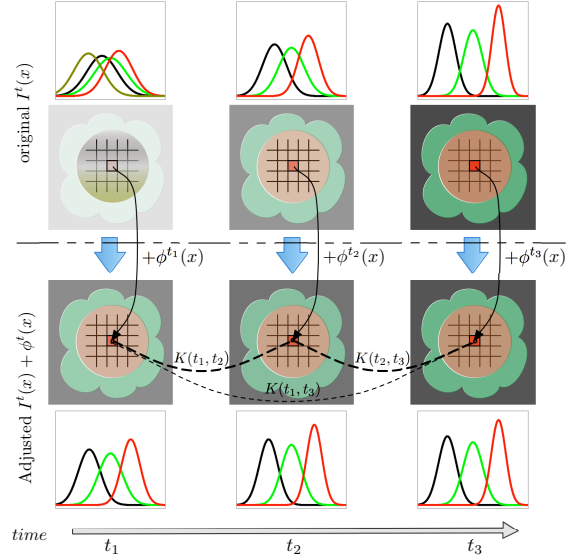


**Fig. 1.** Overview of 4D intensity modeling. Columns from left to right represent time  $t_1$ ,  $t_2$  and  $t_3$ . The first two rows are the original images and their intensity distributions; the last two rows are the adjusted images and new intensity distributions.  $\phi^t(x)$  is the intensity change of voxel  $x$  at time  $t$ .  $K(t_i, t_j)$  is similarity kernel between  $t_i$  and  $t_j$ . Notice at time  $t_1$ , after intensity adjustment, two categories represented by yellow and red merge into one category represented by red.

ference  $d^{(t_i, t_j)}(x) = \|(\mathbf{I}^{t_i}(x) + \phi^{t_i}(x)) - (\mathbf{I}^{t_j}(x) + \phi^{t_j}(x))\|_2$  between time point  $t_i$  and  $t_j$ , where  $\|\cdot\|_2$  is the  $L_2$  norm.

Modeling intensity similarity will be achieved by minimizing the 4D intensity change objective function

$$\mathcal{D}(\phi^t(x)) = \sum_{t_i} \sum_{t_j} K(t_i, t_j) \sum_x (d^{(t_i, t_j)}(x))^2, \quad (1)$$

where  $K(t_i, t_j)$  represents regularization over time, here with a Gaussian kernel like  $K(t_i, t_j) = \exp(-\frac{(t_i - t_j)^2}{\sigma})$ . Notice that the optimization for  $\mathcal{D}(\phi^t(x))$  is 0 in the case that all image intensities are the same after intensity adjustments. To avoid unlimited degrees of freedom for intensity changes, we define constraints with heuristics to be adjusted to the given application domains. To constrain the intensity change  $\phi^t(x)$ , we apply an  $L_1$  penalty for  $\phi^t(x)$ ,

$$\mathcal{R}_1(\phi^t(x)) = \sum_x |\phi^t(x)|. \quad (2)$$

In principle, one could achieve different intensity change constraints for each time point by defining different weights of  $\mathcal{R}_1(\phi^t(x))$ , e.g. with different time spacing. Another penalty to intensity change is spatial smoothness, here modeled by the  $L_2$  norm of the gradients

$$\mathcal{R}_2(\phi^t(x)) = \sum_t \sum_x \|\nabla \phi^t(x)\|^2. \quad (3)$$

The proposed intensity change modeling can deal with both challenges cited above, low contrast changing into higher contrast with well-separated distributions, and inhomogeneities even including multi-modal distributions changing into homogeneous unimodal distributions.

## 2.2. Joint 4D Segmentation

At each time  $t$ , we model each class  $c \in \{1, \dots, C\}$  by a normal distribution with parameters  $\Theta_c^t = \{\mu_c^t, \Sigma_c^t\}$ . Integrating the intensity change model into a longitudinal 4D segmentation, the probability density of adjusted voxel intensity  $\mathbf{I}^t(x) + \phi^t(x)$  attributed to class  $c$  is  $p(\mathbf{I}^t(x) + \phi^t(x) | \Gamma_x^t = c; \Theta_c^t) = \mathcal{N}(\mathbf{I}^t(x) + \phi^t(x); \Theta_c^t)$ , where  $\Gamma_x^t \in \{c | c = 1, \dots, C\}$  is the random variable representing the class  $c$  of voxel at position  $x$  and time  $t$ , and  $\mathcal{N}$  is the normal density function.

Given a prior probability that voxel  $x$  belongs to class  $c$  at time  $t$  as  $p(\Gamma_x^t = c)$  via the image atlas  $A_c^t(x)$ , the overall probability density of voxel intensity  $\mathbf{I}^t(x) + \phi^t(x)$  at position  $x$  and time  $t$  can be calculated by the law of total probability:  $p(\mathbf{I}^t(x) + \phi^t(x); \Theta^t) = \sum_c p(\Gamma_x^t = c) p(\mathbf{I}^t(x) + \phi^t(x) | \Gamma_x^t = c; \Theta_c^t) = \sum_c A_c^t(x) \mathcal{N}(\mathbf{I}^t(x) + \phi^t(x); \Theta_c^t)$ , which is a mixture of normal distributions.

Assuming all voxel intensities of a longitudinal image sequence are statistically independent over time and space, the probability density (likelihood function) of entire image sequence intensity given the mixture of normal model becomes

$$\begin{aligned} \mathcal{L}(\Theta, \phi) &= p(\mathbf{I} + \phi; \Theta) = \prod_t \prod_x p(\mathbf{I}^t(x) + \phi^t(x); \Theta^t) \\ &= \prod_t \prod_x \sum_c A_c^t(x) \mathcal{N}(\mathbf{I}^t(x) + \phi^t(x); \Theta_c^t), \end{aligned} \quad (4)$$

where  $\mathbf{I}$ ,  $\phi$  is the notation for all images intensities and their changes, and  $\Theta$  is representing all parameters of normal distributions over time.

We define our 4D segmentation objective function, which maximizes the likelihood of Eq. 4 and minimizes the intensity change objective defined in Eq. 1, with two the constraints of equations 2 and 3 as follows:

$$\begin{aligned} \mathcal{F}(\phi^t(x), \Theta_c^t) &= -\log \mathcal{L}(\Theta, \phi) + \alpha \mathcal{D}(\phi^t(x)) \\ &+ \sum_t \beta_t \mathcal{R}_1(\phi^t(x)) + \gamma \mathcal{R}_2(\phi^t(x)), \end{aligned} \quad (5)$$

where  $\alpha$ ,  $\beta_t$  and  $\gamma$  are positive parameters. To optimize the segmentation objective function, we use an adaptive gradient descent method to get the optimal  $\phi^t(x)$  and  $\Theta_c^t$  parameters. Finding segmentation is achieved by calculating the posterior probabilities  $p(\Gamma_x^t = c | \mathbf{I}^t(x) + \phi^t(x); \Theta_c^t)$ .

## 3. RESULTS AND DISCUSSION

For synthetic data and clinical data, we use existing probabilistic adult and infant population atlas for white matter, gray matter, csf and remainder classes.

### 3.1. Synthetic Longitudinal Data

We build a synthetic data including 3 time points using BrainWeb's anatomical model of the normal brain as ground truth. To simulate the myelination process of early brain development, we split white matter of the ground truth into myelinated (top) and unmyelinated (bottom) parts at the first time point, as an example for a bimodal distribution within one tissue class. We apply a Gaussian filter with large  $\sigma$  to blur each class, and use the normalized blurred results as the prior probability maps  $p_c^t(x)$ .

The simulated images were generated as  $\mathbf{I}^t(x) = \sum_c p_c^t(x) d_c^t$ , where  $d_c^t \sim \mathcal{N}(\mu_c^t, \Sigma_c^t)$ , i.e. we draw samples from normal distributions and generate simulated image intensities as weighted sums of samples based on the probability maps  $p_c^t(x)$ . We apply statistics from past pediatric imaging research to set parameters  $\mu_c^t, \Sigma_c^t$  (see Fig. 2 for synthetic data and atlas).

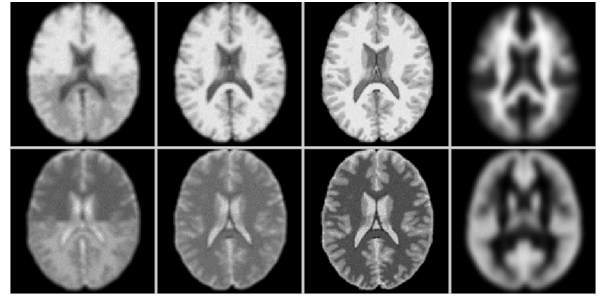


**Fig. 2.** Synthetic data (columns 1-3 from left for time points 1-3; rows 1-2 for modalities 1-2) and Atlas used (column 4 from left-side, rows 1-2 for white and gray matter).

Fig. 3 shows segmentation results and generated intensity changes of the proposed 4D segmentation framework. The intensity change images illustrate a clear compensation for the original images intensities to deal with low contrast. In addition, the two types of white matter, which have different intensity levels and two modes in the intensity distributions, merge into one single tissue type with one single mode. We also compare our proposed 4D segmentation results with a conventional EM segmentation at individual time points to the ground truth. Our proposed segmentation results in significantly improved segmentation in particular at the first and second time points (see Table 1).

### 3.2. Clinical Longitudinal Data

Our new method is also applied to image data from an ongoing clinical infant autism study, here with preliminary tests on 5 subjects with longitudinal multimodal T1w/T2w MRI scanned at 6, 12 and 24 months of age. Whereas the segmentation of the 1 year old scans could be improved as summarized in [2], the segmentation of the 6month old still presented a challenge due to very low contrast, spatial inhomogeneity.

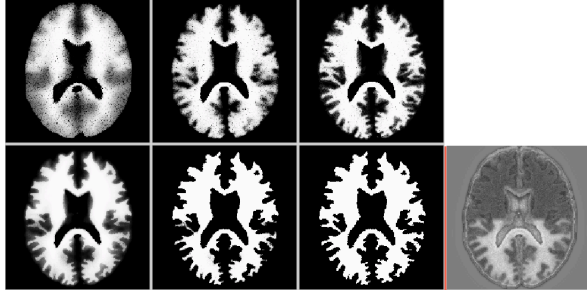


**Fig. 3.** Segmentation of synthetic data (columns 1-3 from left for time points 1-3; row 1 for conventional EM method, row 2 for proposed 4D segmentation) and intensity change of proposed 4D segmentation (column 4, row 2 for modalities 1 at time point 1).

EM/4D	tp	tn	fp	fn	correct
t1	.08/.09	.85/.89	.05/.02	.02/.00	.93/.98
t2	.09/.09	.87/.90	.03/.01	.01/.00	.96/.99
t3	.09/.09	.89/.90	.01/.01	.01/.00	.98/.99

**Table 1.** Quantitative comparison between conventional EM and our proposed 4D segmentation to ground truth of white matter (shown as EM/4D): tp, tn, fp, fn for true positive, true negative, false positive, false negative; correct = tp + tn; t1, t2, t3 for time points 1-3.

geneties and appearance of myelinatend and non-myelinated white matter regions. Moreover, this paper aims at a joint 4D segmentation of all time points rather than independent segmentations of repeated scans per subject. Fig. 4 shows the input MRI data after nonlinear co-registration, and Fig. 5 illustrates the segmentation results for independent time point segmentation (top) and joint 4D segmentation (bottom). A qualitative assessment shows significant improvement of segmentations of the 6 and 12 month’s scans, but quantitative validation via eventually existing manual expert segmentations will be necessary to support this observation.

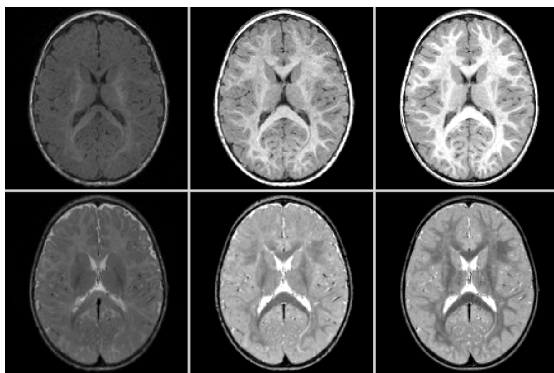


**Fig. 4.** Clinical pediatric scans: columns 1-3 from left: 6, 12 and 24 months of age; rows 1-2 for T1w and T2w axial views.

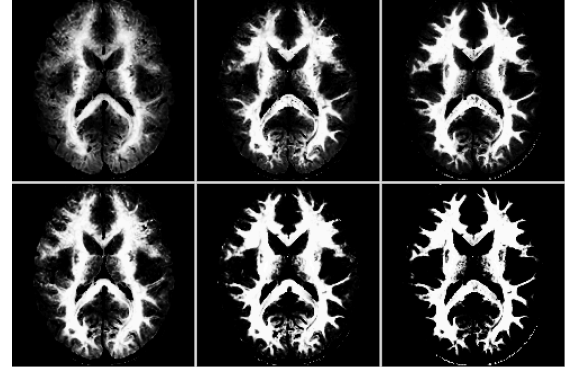


**Fig. 5.** Segmentation of clinical data: columns 1-3 from left-side for 6, 12 and 24 months of age; rows 1 for conventional EM method, row 2 for proposed 4D segmentation.

Whereas this work assumes existing intra-subject nonlinear registration of images across time points, which is much less challenging than inter-subject registration due to high self-similarity of same-subject anatomies, future work will integrate the proposed 4D segmentation based on the new intensity change modeling with co-registration, similar to the framework by [5].

#### 4. REFERENCES

- [1] M. Reuter, N. J. Schmansky, H. D. Rosas, and B. Fischl, “Within-subject template estimation for unbiased longitudinal image analysis,” *NeuroImage*, vol. 61, no. 4, pp. 1402 – 1418, Mar. 2012.
- [2] S. H. Kim, V. S. Fonov, C. Dietrich, and et al., “Adaptive prior probability and spatial temporal intensity change estimation for segmentation of the one-year-old human brain,” *Journal of Neuroscience Methods*, vol. 212, no. 1, pp. 43–55, Jan. 2013.
- [3] F. Shi, Y. Fan, S. Tang, D. Shen, and et al., “Neonatal brain image segmentation in longitudinal MRI studies,” *NeuroImage*, vol. 49, no. 1, pp. 391–400, Jan. 2010.
- [4] Z. Xue, D. Shen, and C. Davatzikos, “CLASSIC: Consistent Longitudinal Alignment and Segmentation for Serial Image Computing,” *NeuroImage*, vol. 30, no. 2, pp. 388–399, Apr. 2006.
- [5] M. Prastawa, S. P Awate, and G. Gerig, “Building spatiotemporal anatomical models using joint 4-D segmentation, registration, and subject-specific atlas estimation,” in *2012 IEEE Workshop on Math. Methods in Biomedical Image Analysis (MMBIA)*. 2012, pp. 49–56, IEEE.
- [6] L. Wang, F. Shi, P-T Yap, J. H Gilmore, W. Lin, and D. Shen, “4D Multi-Modality Tissue Segmentation of Serial Infant Images,” *PLOS ONE*, vol. 7, no. 9, pp. e44596, Sept. 2012.